

# The tumor suppressor p15Ink4b regulates the differentiation and maturation of conventional dendritic cells

Joanna Fares,<sup>1,2</sup> Richard Koller,<sup>1</sup> Rita Humeniuk,<sup>1</sup> Linda Wolff,<sup>1</sup> and Juraj Bies<sup>1</sup>

<sup>1</sup>Laboratory of Cellular Oncology, National Cancer Institute, National Institutes of Health, Bethesda, MD; and <sup>2</sup>Department of Biochemistry, Molecular and Cellular Biology, Georgetown University Medical Center, Washington, DC

**The tumor suppressor p15Ink4b is frequently inactivated by methylation in acute myeloid leukemia and premalignant myeloid disorders. Dendritic cells (DCs) as potent APCs play critical regulatory roles in antileukemic immune responses. In the present study, we investigated whether p15Ink4b can function as modulator of DC development. The expression of p15Ink4b is induced strongly during differentiation and activation of DCs, and its loss resulted in significant**

**quantitative and qualitative impairments of conventional DC (cDC) development. Accordingly, ex vivo-generated BM-derived DCs from p15Ink4b-knockout mice express significantly decreased levels of the antigen-presenting (MHC II) and costimulatory (CD80 and CD86) molecules and have impaired immunostimulatory functions, such as antigen uptake and T-cell stimulation. Reexpression of p15Ink4b in progenitors restored these defects, and confirmed a positive role for**

**p15Ink4b during cDC differentiation and maturation. Furthermore, we have shown herein that p15Ink4b expression increases phosphorylation of Erk1/Erk2 kinases, which leads to an elevated activity of the PU.1 transcription factor. In conclusion, our results establish p15Ink4b as an important modulator of cDC development and implicate a novel function for this tumor suppressor in the regulation of adaptive immune responses. (*Blood*. 2012;119(21):5005-5015)**

## Introduction

In acute myeloid leukemia (AML), one of the most common epigenetic abnormalities observed in patients is the transcriptional silencing of *p15INK4b* (*Cdkn2b*) by DNA hypermethylation.<sup>1,2</sup> Increased DNA methylation of the *p15INK4b* gene regulatory sequences has been reported in up to 80% of all patients suffering from AML, and in a high proportion of patients with other hematologic disorders, including myelodysplastic syndrome (MDS), and myeloproliferative neoplasms.<sup>3,4</sup> Clinical observations have established a strong correlation between the methylation levels of *p15INK4b* and poor prognosis in patients. Hypermethylation also provides a biomarker for the subsequent transformation and progression of the disease to a more aggressive phenotype.<sup>3</sup> The tumor-suppressor function of p15Ink4b for myeloid diseases was confirmed experimentally in an animal model with myeloid-specific deletion of the gene. These mice suffer from a mild form of myeloproliferative neoplasm resembling chronic myelomonocytic leukemia and are strongly predisposed to retrovirus-induced AML.<sup>5</sup>

p15INK4b is a cyclin-dependent kinase inhibitor (CDKI) that binds and inhibits the activity of 2 cyclin-dependent kinases, CDK4 and CDK6. This inhibition leads to cell-cycle arrest during the early and mid-G<sub>1</sub> phase.<sup>6</sup> In accordance with its cell cycle-inhibitory function, the expression levels of p15Ink4b are reported to be increased during the late maturation stages of myeloid progenitors associated with terminal differentiation into macrophages.<sup>7</sup> p15Ink4b has also been shown to play a role during early stages of hematopoiesis independently from its cell cycle-inhibitory function.<sup>8</sup> During early myeloid-cell development, the loss of p15Ink4b in knockout mice favors the differentiation of common myeloid progenitors (CMPs) into granulocyte macro-

phage progenitors (GMPs), resulting in an imbalance between the erythroid and myeloid compartments.<sup>8</sup>

During leukemogenesis, an important step in the establishment and progression of disease, is evasion of the preleukemic/leukemic cells from efficient surveillance and clearance by the immune system. The critical players in the initiation of immune surveillance and the maintenance of self-tolerance are the dendritic cells (DCs).<sup>9,10</sup> DCs function primarily as APCs that have the exclusive capacity of stimulating naive T cells against pathogens and cancerous cells. Recent studies have established DCs as a distinct hematopoietic lineage.<sup>11</sup> Differentiation steps include the macrophage-DC progenitors (MDPs), that are derived from CMPs and give rise to the common DC precursors (CDPs).<sup>12,13</sup> This differentiation scheme suggests that myeloid precursors of CDPs also include preleukemic/leukemic progenitors with genetic/epigenetic changes that may hamper their differentiation/maturation into fully functional DCs necessary for efficient antileukemic immune response.<sup>14,15</sup>

Previous studies have implicated a role for p15Ink4b during normal myeloopoiesis and in myeloid diseases; however, its potential function in the differentiation and maturation of DCs has not been addressed. Using the p15Ink4b<sup>fl/fl</sup>/LysMcre conditional knockout mouse model developed previously in our laboratory,<sup>5</sup> in the present study, we show that the loss of p15Ink4b affects the differentiation and maturation of conventional DCs (cDCs) in vivo and ex vivo. The p15Ink4b-deficient mice have substantially reduced numbers of CDPs, and spleen and BM cDCs. Ex vivo-generated BM-DCs from the knockout mice have markedly lower levels of expression of MHC II, and the costimulatory molecules CD80 and CD86 than wild-type controls. Accordingly,

Submitted October 24, 2011; accepted March 23, 2012. Prepublished online as *Blood* First Edition paper, March 28, 2012; DOI 10.1182/blood-2011-10-387613.

The online version of this article contains a data supplement.

The publication costs of this article were defrayed in part by page charge payment. Therefore, and solely to indicate this fact, this article is hereby marked "advertisement" in accordance with 18 USC section 1734.

these cells show a reduced ability to uptake antigen and to stimulate allogeneic T-cell responses. The reexpression of p15Ink4b in progenitors resulted in a restoration of MHC II expression and costimulatory molecules, confirming a positive role for p15Ink4b in cDC development. Furthermore, we have shown herein that p15Ink4b expression increases the phosphorylation of Erk1/Erk2 protein kinases that leads to an increased transactivation activity of the PU.1 transcription factor, an important regulator of DC development.

Our present results establish the tumor suppressor p15Ink4b as an important modulator of cDC development and suggest that the loss of its expression due to promoter methylation or gene deletion may result in less effective adaptive immune responses.

## Methods

### Mice

The generation and characterization of conditional and embryonal p15Ink4b-knockout mice have been described previously.<sup>5,16</sup> Handling and treatment of mice were performed in accordance with animal protocols approved by the National Institutes of Health (NIH) Intramural Animal Care and Use Committee.

### Cells

BM-DCs were generated as described previously.<sup>17,18</sup> Briefly, BM cells were cultured in IMDM containing 10% FCS, 2mM glutamine, and 100 U of penicillin/streptomycin supplemented with 20 ng/mL of recombinant murine GM-CSF and 10 ng/mL of IL-4 (PeproTech). The cells were seeded at a density of  $5 \times 10^5$  cells/mL and 50% of the medium was replaced with fresh cytokine-containing medium on days 3 and 5. BM-DC culture on day 5 had approximately 70% CD11c<sup>+</sup>CD11b<sup>+</sup>CD8 $\alpha$ <sup>-</sup> BM-DCs and were activated/matured by overnight treatment with lipopolysaccharide (LPS) treatment 100 ng/mL; *Escherichia coli* serotype 0127:B8; Sigma-Aldrich). For analysis of splenic DCs, splenocytes were isolated from the mice, dissected, and incubated in serum-free RPMI containing 400 U/mL of collagenase I and 20  $\mu$ g/mL of DNase I (Roche) for 1 hour at 37°C. DCs were enriched using a custom negative-enrichment cocktail (StemCell Technologies) according to the manufacturer's protocol. Hematopoietic progenitors were isolated from the BM using the EasySep Mouse Hematopoietic Progenitor Cell Enrichment Kit (StemCell Technologies). Dr Cynthia Dunbar (Hematology Branch, National Heart, Lung and Blood Institute, NIH, Bethesda, MD) generously provided human CD34<sup>+</sup> cells from healthy donors.

### Flow cytometry

The Abs used for flow cytometric analysis and cell sorting are listed in supplemental Table 1 (available on the *Blood* Web site; see the Supplemental Materials link at the top of the online article). Cells ( $5-10 \times 10^6$  cells/mL) were incubated for 30 minutes in the dark at room temperature with a cocktail of mAbs. For intracellular cytokine staining, Golgi Stop reagent (BD Pharmingen) was added to the cells simultaneously with LPS. After an 8-hour activation period, cells were first stained with Abs against surface molecules and then fixed and permeabilized with Cytofix/Cytoperm (BD Pharmingen) according to the manufacturer's protocol. Data collection was performed on a FACSCanto II or an LSR II flow cytometer (BD Biosciences). Analysis was performed using FlowJo Version 7.5.5 software (TreeStar). Cell sorting was done on the FACSaria III cell sorter (BD Biosciences).

### Cell lines and plasmid constructs

The murine cell line M1 and RAW264.7 cells were maintained as described previously.<sup>5,19</sup> Vector expressing DDp15Ink4b under the control of the destabilizing domain (DD) was constructed by first inserting murine

*p15Ink4b* cDNA into the EcoR-I and Not-I sites of pLVX-PTuner vector (Clontech). The DDp15Ink4b sequence was then amplified using primers *XhoI*-DD (ATCCTCGAGCATGGGAGTGCAGGTGG) and *HpaI*-p15 (GTAACTTCAATCTCCAGTGGCAGC) and subcloned into the *XhoI* and *HpaI* sites of a retroviral vector pMSCV-IRES-GFP (Mig). RAW 264.7 cells or enriched hematopoietic progenitors were infected with an empty viral Mig vector (Mig0) or Mig expressing DD-p15Ink4b (MigDDp15) retroviruses in the presence of 5  $\mu$ g/mL of polybrene (Sigma-Aldrich) by 2 rounds of spinoculation at 485g for 1 hour. Forty-eight hours after infection, green fluorescent protein-expressing cells were sorted, expanded in IMDM supplemented with murine SCF, murine IL-3, and murine IL-6 (PeproTech) and differentiated into BM-DCs with GM-CSF and IL-4.

### Allogeneic T-cell proliferation assay

Balb/c T cells were purified following the EasySep negative selection protocol (StemCell Technologies), and then stained with fluorescent CFSE dye as described previously.<sup>20</sup> Briefly, T cells were resuspended at  $10^6$  cells/mL in PBS and incubated at 37°C for 7 minutes with 0.5  $\mu$ M CFSE (Molecular Probes). After the addition of serum and 2 PBS washes, CFSE-labeled T cells were cultured at a density of  $10^5$  cells/well in 96-well U-bottom plates (Falcon) with various numbers of sorted CD11c<sup>+</sup>CD11b<sup>+</sup> DCs. Cells were kept at 37°C in 5% CO<sub>2</sub> for 5 days and analyzed on day 5 by FACS.

### Antigen uptake

To measure antigen uptake, BM-DCs were incubated with 1  $\mu$ g/mL of FITC-labeled ovalbumin peptide (OVA; Molecular probes) at 4°C (background control) or 37°C. Cells were collected at the indicated time points and the incorporation of FITC-OVA into CD11c<sup>+</sup>CD11b<sup>+</sup> cells was monitored by flow cytometry.

### RNA isolation and qPCR

Total RNA was prepared according to the miRCURY RNA isolation kit (Exiqon) protocol. cDNA was produced from 1  $\mu$ g of total RNA using the RNA-to-cDNA reverse transcription kit (Applied Biosystems). Real-time quantitative PCR (qPCR) was performed in triplicate using one-tenth the cDNA reaction with predesigned gene-expression assays (Applied Biosystems) for mouse *p15Ink4b* (Mm00483241) and *Gapdh* (4352932) and for human *p15INK4b* (Hs00793225) and *18S RNA* (4333760). Relative quantitation was carried out by the comparative threshold cycle ( $C_T$ ) method. *p15Ink4b* genomic DNA copy number was performed using custom primer and probe sets against the floxed exon 2 and calculated using exon 1 of the gene for normalization (supplemental Table 2).

### Statistical analysis

Statistical analysis was performed using Prism Version 5 software (GraphPad) using an unpaired 2-tailed Student *t* test on measurements of experimental replicates. For gene expression, relative quantitation was carried out with the  $C_T$  method.<sup>21</sup>

### Western blot analysis

Cells were disrupted in ice-cold lysis buffer supplemented with Protease & Phosphatase Inhibitor Cocktail (Halt; Thermo Scientific). Whole-cell lysates were fractionated by SDS-PAGE on a 4%-12% gradient gel and transferred electrophoretically to a nitrocellulose membrane. Immunoblots were blocked, incubated with Abs, and visualized with SuperSignal West Pico chemiluminescent substrate (Pierce) in accordance with the manufacturer's instructions.

### ChIP assay

For detection of proteins bound to DNA in vivo, the SimpleChIP enzymatic Chromatin IP Kit (Cell Signaling Technology) was used in accordance with the manufacturer's protocol. Cross-linked chromatin was digested with

micrococcal nuclease and immunoprecipitated with ChIP-formulated Abs: PU.1, histone H3, and normal rabbit IgG (Cell Signaling Technology). Immunoprecipitated DNA was amplified by qPCR using primers/probe sets specific for the CD80 and CD86 promoters<sup>22</sup> (see supplemental Table 2). Two independent experiments were performed in triplicate for each ChIP. Results were normalized to H3 control enrichment and graphed as the -fold increase in enrichment over normal IgG ChIPs.

### Luciferase assay

Raw264.7 cells ( $2 \times 10^6$  cells/mL) were washed in PBS, resuspended in 100  $\mu$ L of Nucleofector Kit V (Lonza) supplemented with 2  $\mu$ g of Pu.1-dependent luciferase reporter construct (pPU.1-Luc)<sup>23</sup> and 30 ng of *Renilla* luciferase pCMV-RL (Promega) control construct for normalization, and transfected by electroporation using Nucleofector II (Lonza). Luciferase activity was assessed using the Dual-Luciferase Reporter System (Promega) and the TurnerTD-20e luminometer.

## Results

### Differentiation and maturation of cDCs are accompanied by a transcriptional up-regulation of *p15Ink4b*

To assess whether p15Ink4b could play a role in the development and activation of DCs, we first analyzed expression of *p15Ink4b* mRNA in cDCs compared with hematopoietic c-Kit<sup>+</sup> progenitors. FACS plots of enriched hematopoietic progenitors and enriched splenic DCs, as well as the gating strategy for FACS sorting of c-Kit<sup>+</sup> and CD11c<sup>+</sup>CD11b<sup>+</sup> cDCs, are shown in Figure 1A. PCR analyses revealed that the level of *p15Ink4b* mRNA expression in cDCs was strongly elevated (> 300-fold) compared with c-Kit<sup>+</sup> BM cells (Figure 1B). To investigate *p15Ink4b* mRNA expression throughout the maturation and activation of DCs, we generated BM-DCs (CD11c<sup>+</sup>CD11b<sup>+</sup>) in vitro from BM cells cultured in the presence of GM-CSF and IL-4.<sup>17</sup> BM-DCs were sorted and activated or not activated with LPS (Figure 1C). Consistent with the results from splenic cDCs, *p15Ink4b* mRNA was strongly induced in the immature BM-DCs compared with c-Kit<sup>+</sup> cells when FACS sorted from lineage-negative hematopoietic progenitors and further up-regulated after stimulation with LPS (Figure 1D). The biphasic up-regulation of *p15Ink4b* expression was also confirmed in human DCs generated from CD34<sup>+</sup> human hematopoietic cells<sup>24</sup> activated with LPS (Figure 1E-G). These results suggest an important role for p15Ink4b during the development and the activation of DCs.

### Loss of p15Ink4b in vivo results in a reduction of CDP populations in BM

The role of p15Ink4b as a tumor suppressor for myeloid malignancies was first demonstrated experimentally using the p15Ink4b<sup>fl/fl</sup>LysMcre conditional mouse model, in which *p15Ink4b* deletion is restricted to cells of the myeloid lineage.<sup>5</sup> The absence of p15Ink4b in these mice results in increased GMP production at the expense of megakaryocyte/erythroid progenitors and leads to monocytosis in the peripheral blood and BM.<sup>5</sup> To determine whether absence of p15Ink4b also affects the early DC progenitor (CDP) populations, BM cells were analyzed by FACS. The gating strategy used to identify the Flt3<sup>+</sup>c-kit<sup>int</sup>M-CSFR<sup>+</sup> CDPs was performed as described previously<sup>13,25</sup> and is depicted in Figure 2A. Surprisingly, we detected a significant decrease in the percentage and total cell numbers of CDPs in p15Ink4b<sup>fl/fl</sup>LysMcre mice compared with p15Ink4b<sup>w/w</sup>LysMcre control mice, whereas the multipotent progenitors (MPPs; Flt3<sup>-lo</sup>c-kit<sup>hi</sup>/M-CSFR<sup>-</sup>) were not

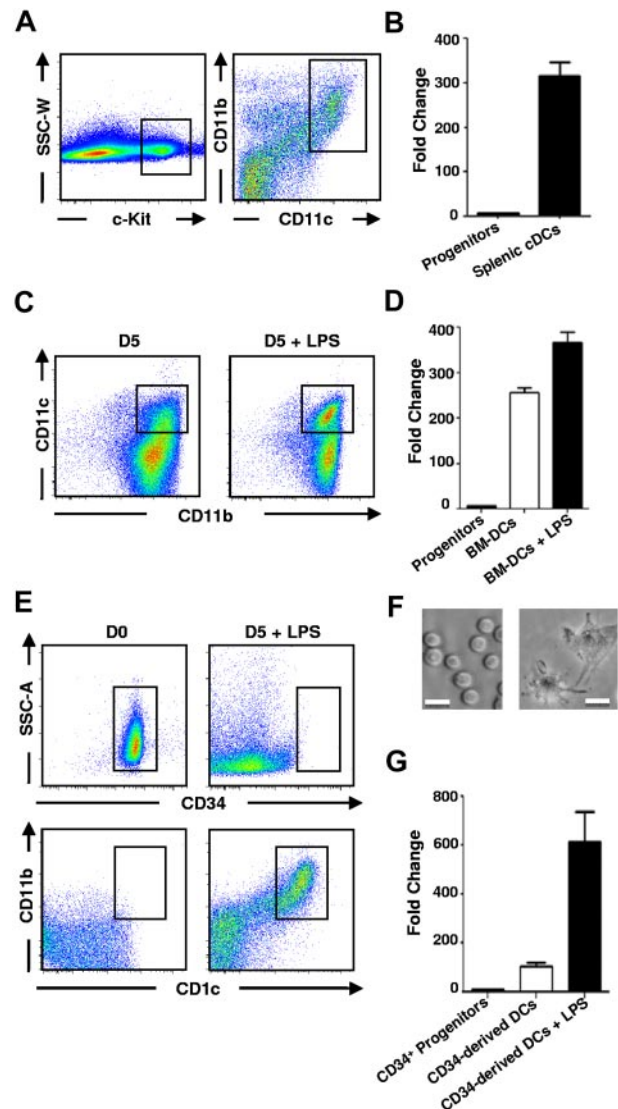
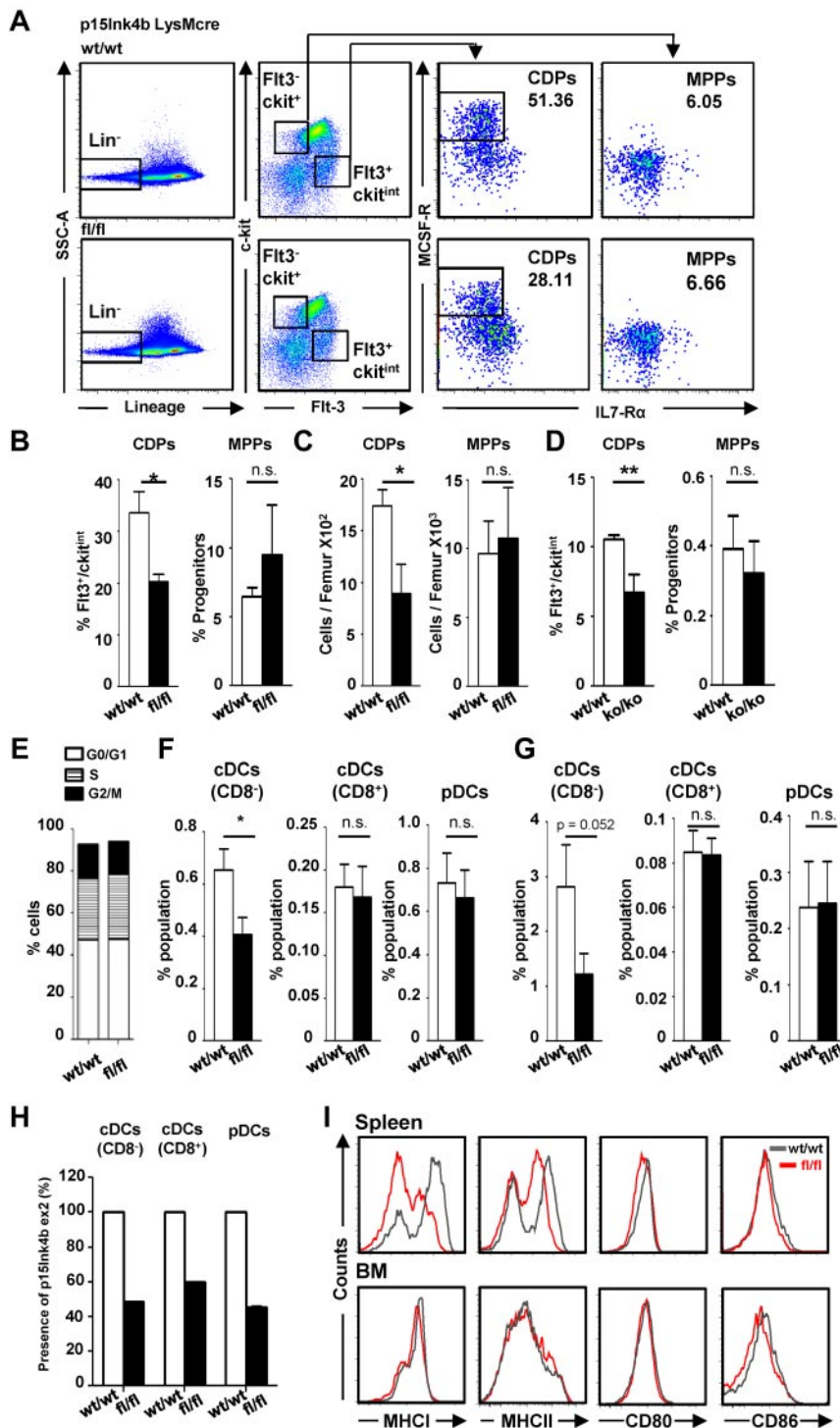


**Figure 1. Increased expression of *p15Ink4b* mRNA in cDCs.** (A) FACS plots depicting the gating strategy for FACS sorting of mouse FACS-sorted c-Kit<sup>+</sup> cells from lineage-negative enriched BM progenitors (left) and CD11c<sup>+</sup>/CD11b<sup>+</sup> splenic cDCs from enriched splenic DCs (right). DCs were enriched using a negative-enrichment cocktail containing biotinylated Abs against murine CD2, CD90.2, CD19, Ly-6G, and TER-119. (C) CD11c<sup>+</sup>CD11b<sup>+</sup> BM-DCs from the GM-CSF and IL-4 BM cultures. (B,D,G) Real-time qPCR analysis of *p15Ink4b* mRNA levels of the sorted populations of cells. (E) Human CD34<sup>+</sup> progenitors and CD34-derived CD11c<sup>+</sup>CD11b<sup>+</sup> cDCs. Cells were harvested at the indicated time points. (F) Bright-field images of human CD34<sup>+</sup> progenitors (left) and CD34-derived DCs on day 5 of culture (right). Scale bar represents 20  $\mu$ m. Images were collected using an Olympus iX51 inverted microscope, a EXi Aqua Camera (QImaging), and the acquisition software IPlab Version 4.08 (BD Biosciences), and were processed in Adobe Photoshop Version 5.0.

affected (Figure 2B-C). Deletion efficiency of *p15Ink4b* in FACS-sorted CDPs was assessed by qPCR to be approximately 35% (data not shown). FACS analyses of lineage-negative BM cells isolated from p15Ink4b embryonal-knockout mice with a complete deletion of *p15Ink4b*<sup>8</sup> revealed an even more significant decrease of CDPs in knockout mice (Figure 2D). To investigate whether deletion of *p15Ink4b* affects the cycling capacity of CDPs, we analyzed by FACS 7AAD-stained CDP populations isolated from wild-type or floxed mice. Our results revealed a similar distribution of cells in each phase of the cell cycle (Figure 2E), suggesting that the cycling frequency of DC progenitors is not affected by the loss of p15Ink4b.





### Reduction of cDCs in the BM and spleen of *p15Ink4b*-deficient mice

We also investigated the impact of *p15Ink4b* deletion on the more differentiated subsets of DCs in the BM and spleen. Flow cytometric analyses of cells from *p15Ink4b<sup>fl/fl</sup>LysMcre* and *p15Ink4b<sup>wt/wt</sup>LysMcre* mice revealed a significant reduction of CD8 $^{-}$  cDCs (CD11c $^{+}$ CD11b $^{+}$ CD8 $^{-}$ ) in the spleen and BM of the *p15Ink4b<sup>fl/fl</sup>LysMcre* mice, but not the CD8 $^{+}$  cDCs (CD11c $^{int}$ CD11b $^{-}$ CD8 $^{+}$ ) or plasmacytoid DC (pDC) (CD11c $^{+}$ CD11b $^{-}$ CD8 $^{-}$ B220 $^{+}$ ) populations (Figure 2F-G). Interestingly, deletion efficiencies of *p15Ink4b* exon 2 were similar in all

3 DC populations (Figure 2H), suggesting subset specific regulation of DCs by *p15Ink4b*. These results were confirmed in BM isolated from mice with an embryonic knockout of *p15Ink4b*, in which we again detected a significant decrease only in the CD8 $^{-}$  cDC populations in knockout mice; the CD8 $^{+}$  cDC numbers were not affected and the pDC numbers were actually increased (supplemental Figure 1). Immature DCs express MHC I and MHC II molecules and are characterized by high antigen capture and processing capacities,<sup>26-28</sup> whereas mature DCs up-regulate the levels of the costimulatory molecules CD80 and CD86, which are

**Figure 2. Decreased CDPs and CD8 $^{-}$  cDCs in *p15Ink4b<sup>fl/fl</sup>LysMcre* mice.** (A) Flow cytometry and gating strategy of lineage-negative enriched mouse progenitors to identify  $Fit3^{+}$ M-CSFR $^{-}$  CDPs and  $Fit3^{-}$ M-CSFR $^{-}$  multipotent progenitors. Percentages (B) and total cell numbers (C) of CDPs and multipotent progenitors (MPPs) in *p15Ink4b<sup>wt/wt</sup>LysMcre* mice (wt/wt, n = 6) and *p15Ink4b<sup>fl/fl</sup>LysMcre* mice (fl/fl, n = 6). (D) Percentages of CDPs and multipotent progenitors in wild-type (wt/wt) and embryonic *p15Ink4b* knockout (ko/ko) mice. Data are shown as means  $\pm$  SD. (E) Cell-cycle distribution of CDPs isolated from *p15Ink4b<sup>wt/wt</sup>LysMcre* mice (wt/wt) and *p15Ink4b<sup>fl/fl</sup>LysMcre* mice (fl/fl) mice. Frequency of CD8 $^{-}$  cDCs (defined here as CD11c $^{+}$ CD8 $^{-}$ CD11b $^{+}$ ) CD8 $^{+}$  cDCs (CD11c $^{+}$ CD8 $^{+}$ CD11b $^{-}$ ) and pDCs (CD11c $^{+}$ B220 $^{+}$ CD11b $^{-}$ ) in the spleen (F) and BM (G) of *p15Ink4b<sup>wt/wt</sup>LysMcre* (wt/wt, n = 9) and *p15Ink4b<sup>fl/fl</sup>LysMcre* (fl/fl, n = 9) mice.  $2 \times 10^6$  events were acquired for each sample. (H) Efficiency of *LysMcre*-driven deletion of *p15Ink4b* in FACS-sorted CD8 $^{-}$  cDCs, CD8 $^{+}$  cDCs, and pDCs isolated from *p15Ink4b<sup>wt/wt</sup>LysMcre* and *p15Ink4b<sup>fl/fl</sup>LysMcre* mice. DNA was analyzed by qPCR for the *p15Ink4b* exon 2 copy number with *p15Ink4b* exon 1 used as an internal control. (I) Expression of MHC I, MHC II, CD80, and CD86 molecules on steady-state cDCs from spleen (Sp) and BM of *p15Ink4b<sup>wt/wt</sup>LysMcre* (black line) and *p15Ink4b<sup>fl/fl</sup>LysMcre* mice (red line). The results are representative histograms of 4 independent experiments with similar results. \* $P < .05$ ; \*\* $P < .01$ ; n.s. indicates not significant.

required for effective stimulation of T cells. To determine whether p15Ink4b affects the expression of cell-surface molecules, we performed FACS analyses on DCs enriched from the BM and spleen. As expected, FACS analysis of steady-state splenic and BM immature cDCs revealed very low levels of CD80 and CD86 in both p15Ink4b<sup>fl/fl</sup>LysMcre and p15Ink4b<sup>wt/wt</sup>LysMcre mice. However, splenic cDCs from p15Ink4b<sup>fl/fl</sup>LysMcre mice showed a lower expression of MHC I and MHC II compared with p15Ink4b<sup>wt/wt</sup>LysMcre mice (Figure 2I), suggesting that the antigen-presenting capacities of these cells might be affected by the loss of p15Ink4b.

### Loss of p15Ink4b decreases the capacity of cDCs to up-regulate MHC II and costimulatory molecules after activation

To investigate the role of p15Ink4b in the maturation process of cDCs, we generated DCs *in vitro* from BM cells cultured in medium supplemented with GM-CSF and IL-4. Efficient deletion of the *p15Ink4b* exon 2 (Figure 3A) in cells generated from floxed mice was detected by qPCR and confirmed by Western blot analyses (Figure 3B). Loss of p15Ink4b in LPS-activated BM-DCs from floxed mice resulted in significantly decreased numbers of BM-DCs expressing high levels of MHC II, CD80, and CD86 (Figure 3C). Evaluation of the mean fluorescence intensity (MFI) of positive cells revealed that the BM-DCs from floxed mice expressed substantially lower levels of MHC II, CD80, and CD86 than cells from wild-type mice, indicating a less mature phenotype (Figure 3D). Similar results were obtained with poly(I:C), another potent activator of DCs (data not shown). These results suggest that p15Ink4b is required for optimal maturation of DCs.

### Loss of p15Ink4b results in a reduction of the immunostimulatory functions of cDCs

Reduced levels of MHC II expression in steady-state splenic cDCs and BM-DCs isolated from p15Ink4b-floxed mice are indicative of a poorly differentiated phenotype. Therefore, we investigated whether the other functions of immature cDCs, such as antigen uptake, were also affected by the loss of p15Ink4b. As shown in Figure 4A, p15Ink4b<sup>fl/fl</sup>LysMcre-derived BM-DCs were able to internalize antigen (OVA-FITC) less efficiently than p15Ink4b<sup>wt/wt</sup>LysMcre-derived BM-DCs. As shown in Figure 4B, a significantly decreased antigen-uptake capability in p15Ink4b<sup>fl/fl</sup>LysMcre BM-DCs was detected within 30 minutes of incubation and maintained over the course of the experiment. Intracellular localization of OVA-FITC peptides was confirmed by fluorescent confocal microscopy (supplemental Figure 2). Because treatment of p15Ink4b<sup>fl/fl</sup>LysMcre BM-DCs with LPS results in a lower expression of CD80 and CD86 compared with control BM-DCs, we investigated their ability to stimulate allogeneic T cells from Balb/c mice. BM-DCs derived from floxed and wild-type mice were used in a mismatched T-cell activation assay. As shown in Figure 4C, p15Ink4b<sup>fl/fl</sup>LysMcre BM-DCs had a significantly lower capacity to stimulate the proliferation of allogeneic T lymphocytes compared with the p15Ink4b<sup>wt/wt</sup>LysMcre BM-DCs.

FACS analyses also revealed that BM-DCs derived from floxed mice produced significantly lower levels of the proinflammatory TNF- $\alpha$ , but not IL-12 (Figure 4D). Production of the anti-inflammatory cytokine IL-10 was only slightly increased (Figure 4E).

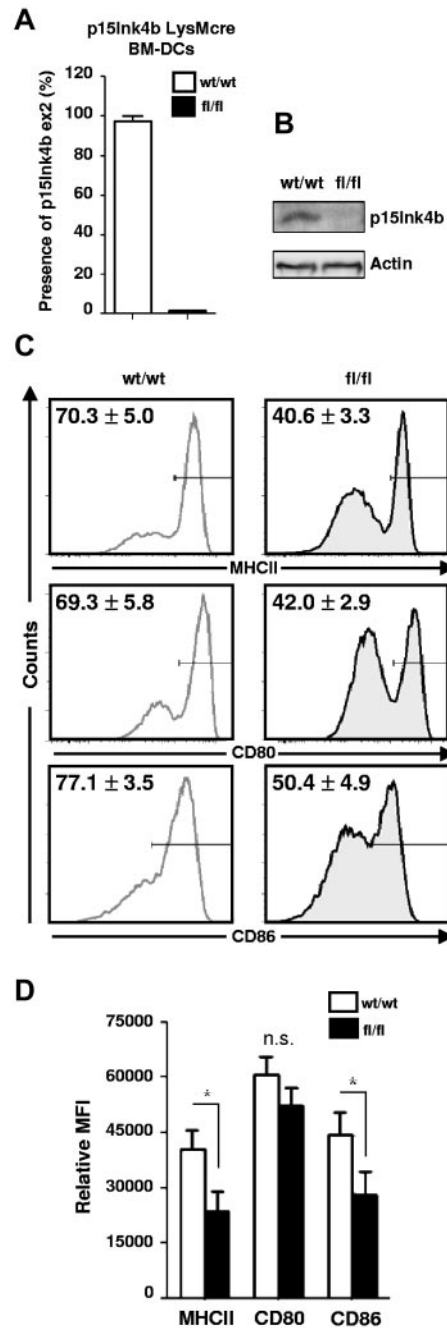


**Figure 3. LysMCre-driven deletion of *p15Ink4b* in BM-DCs impairs their maturation.** (A) Efficiency of LysMCre-driven deletion of p15Ink4b in sorted, LPS-treated BM-DCs derived from p15Ink4b<sup>wt/wt</sup>-LysMcre and p15Ink4b<sup>fl/fl</sup>-LysMcre mice. DNA was analyzed by qPCR for the *p15Ink4b* exon2 copy number, with *p15Ink4b* exon 1 used as an internal control. (B) Western blot of LPS-treated BM-DCs probed with anti-p15Ink4b Ab. For a loading control, the same blot was stripped and reprobed with anti-actin Ab. (C) LPS-treated BM-DCs from p15Ink4b<sup>wt/wt</sup>-LysMcre (wt/wt; left panel) and p15Ink4b<sup>fl/fl</sup>-LysMcre mice (fl/fl; right panel) were analyzed by FACS for the expression of MHC II, CD80, and CD86 molecules. Numbers in histograms indicate percentages of positive staining from 3 independent experiments (n = 7 for each genotype). (D) Bar graphs depicting the relative mean fluorescence intensity values of MHC II, CD80, and CD86 expression on gated positive populations of BM-DCs. Data are shown as means ± SD. \*P < .05; n.s. indicates not significant.

### Reexpression of p15Ink4b reverses differentiation and maturation defects of BM-DCs

To confirm that defects in cDCs are specific for the loss of p15Ink4b, we restored the expression of p15Ink4b in cells and

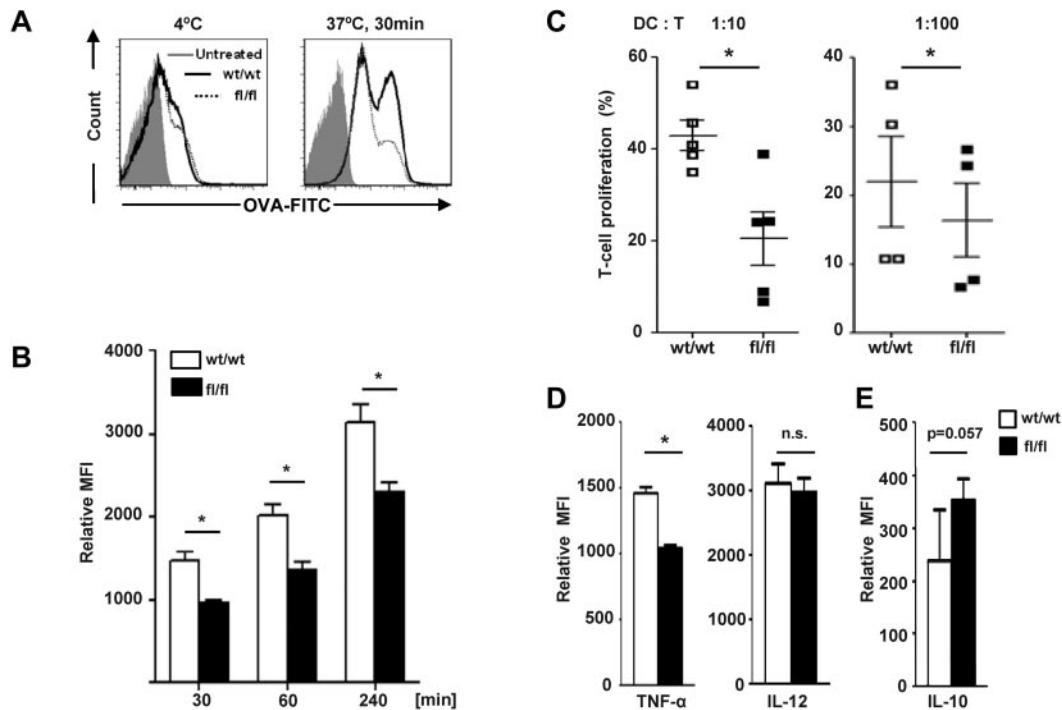


**Figure 4. *p15Ink4b*-deficient BM-DCs have decreased immunostimulatory functions.** (A) BM-DCs were cultured at 37°C in the presence of FITC-labeled OVA antigen. Cells incubated at 4°C for 30 minutes with FITC-labeled OVA antigen were used as a negative control. Representative histograms at the 30-minute time point are shown. (B) BM-DCs from *p15Ink4b*<sup>wt/wt</sup>-LysMcre (*wt/wt*) or *p15Ink4b*<sup>fl/fl</sup>-LysMcre (*fl/fl*) mice were harvested at the indicated times after culture in the presence of OVA. Mean fluorescence intensity values are indicated. (C) BM-DCs from *wt/wt* or *fl/fl* mice were mixed with CFSE-labeled allogeneic T lymphocytes (ratio 1:10 and 1:100) and cocultured for 5 days. T-cell proliferation was assessed using flow cytometry. Numbers indicate the percentage of CFSE<sup>low</sup> T cells. Data are shown as means ± SD from 3 independent experiments. (D-E) BM-DCs were activated with LPS (100 ng/mL) in the presence of GolgiStop (BD Biosciences) for 6 hours, stained for surface molecules that were CD11c<sup>+</sup>CD11b<sup>+</sup>, and then analyzed for the expression of TNF-α, IL-12 (D), and IL-10 (E). Cells were fixed and permeabilized according to the BD Cytotfix/Cytoperm (BD Biosciences) protocol. Relative mean fluorescence intensity values from 2 independent experiments (n = 4) are plotted. Data are shown as means ± SD. \*P < .05; n.s. indicates not significant.

investigated whether defects in differentiation and maturation/activation of cDCs can be reversed. For stable expression of *p15Ink4b*, we used the ProteoTuner system (Clontech), in which a DD fused to *p15Ink4b* (DDp15) causes an increased proteolytic turnover that ensures a low level of expression that can be modulated by binding of a small molecule called Shield-1 (Sh).<sup>28</sup> This system was tested in the RAW264.7 macrophage cell line, which does not express *p15Ink4b* and has been shown to acquire a DC-like morphology and express some DC surface markers, such as CD11c, after treatment with LPS<sup>29,30</sup> (supplemental Figure 3). The experiments in RAW264.7 cells proved that this expression system is suitable for low, physiologically relevant levels of *p15Ink4b* in hematopoietic cells. Reexpression of *p15Ink4b* in primary BM-DCs resulted in a significantly larger fraction of the MigDDp15 progenitors differentiated into BM-DCs (65%) compared with the Mig0 progenitors (32%; Figure 5A). The enhanced potential of progenitors expressing MigDDp15 to differentiate into BM-DCs was also confirmed by light microscopy, which showed that cells expressing DDp15 underwent a remarkable morphological transformation and acquired a DC-like morphology (Figure 5B). BM-DCs infected with MigDDp15 also expressed considerably higher levels of MHC II and the costimulatory molecules CD80, CD86, and CD40 compared with cells infected with Mig0 (Figure 5C-D). These results provide clear evidence that reexpression of *p15Ink4b* in hematopoietic progenitors is able to restore the differentiation/maturation defects observed in cDCs isolated from mice with deleted endogenous *p15Ink4b*.

#### Increased activity of the PU.1 transcription factor in *p15Ink4b*-expressing cells

To gain insight into the molecular mechanism through which *p15Ink4b* can modulate the differentiation and maturation of cDCs, we compared the activation and expression of 2 transcription factors, NFκB and PU.1, known to play a critical role in the regulation of expression of costimulatory molecules.<sup>31-33</sup> RAW264.7 cells infected with Mig0 or MigDDp15 were treated for various times with LPS and analyzed by Western blot. IκBα, an inhibitor of NFκB, was strongly phosphorylated and rapidly degraded after 6 minutes of LPS treatment, and the phosphorylation of NFκB was correlated exactly with degradation of the inhibitor. We did not detect any differences in activation of the NFκB–signaling pathway in cells expressing or not expressing *p15Ink4b* (Figure 6A). Similarly, we did not detect any significant difference in PU.1 protein levels. It was reported recently that PU.1 plays a critical role in the transcriptional regulation of the steady-state level of CD80 and CD86.<sup>22</sup> Therefore, we assessed binding of PU.1 to both promoters in vivo using ChIP analysis. Chromatin complexes were immunoprecipitated from cells using anti-PU.1 and anti-H3 Abs and analyzed by qPCR with CD80- or CD86-specific primers. Increased PU.1 binding to the CD80 and CD86 promoters was detected in cells expressing DDp15 compared with control (Figure 6B). We then evaluated the transactivation activity of PU.1 in cells transfected with a luciferase reporter construct harboring PU.1-binding



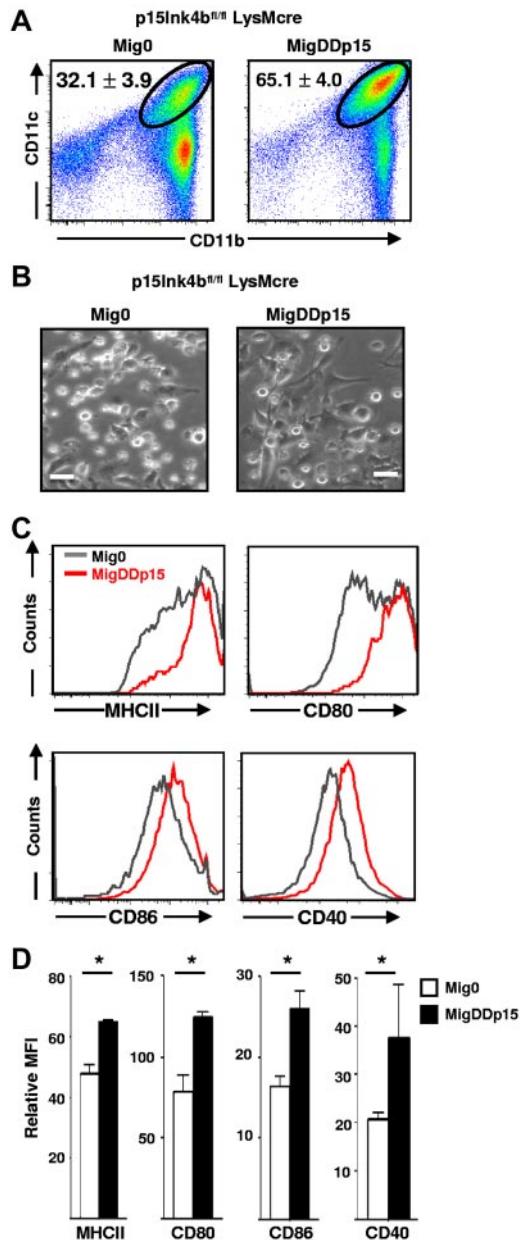


**Figure 5. Reexpression of p15Ink4b results in increased differentiation and maturation of BM-DCs.** (A) Lineage-negative cells from p15Ink4b<sup>fl/fl</sup>-LysMcre mice were infected with Mig0- or MigDDp15-expressing viruses, FACS sorted for GFP<sup>+</sup> cells, and cultured in the presence of GM-CSF (20 ng/mL) and IL-4 (10 ng/mL) for 5 days to generate BM-DCs, which were then FACS analyzed for expression of CD11c and CD11b. Numbers indicate the percentage of double-positive cells ± SD from 2 independent experiments. (B) Bright-field images of the cells on day 5 of culture. Scale bars represent 10  $\mu$ m. (C) BM-DCs were FACS analyzed after treatment with LPS (100 ng/mL for 16 hours) for expression of MHC II, CD80, CD86, and CD40 molecules. (D) Bar graphs depicting relative mean fluorescence intensity values of MHC II, CD80, CD86, and CD40 expression on BM-DCs derived from p15Ink4b<sup>fl/fl</sup>-LysMcre progenitors infected with Mig0 MigDDp15. Data are shown as means ± SD of 2 independent experiments. \* $P < .05$ .

sites.<sup>22</sup> Interestingly, transactivation activity of PU.1 was considerably higher in cells expressing DDp15 compared with control cells regardless of whether they were treated with LPS (Figure 6C). These experiments identified the PU.1 transcription factor as one of the critical downstream executors for p15Ink4b, showing it to be responsible for the increased expression of CD80 and CD86 in cells.

### Elevated phosphorylation of Erk kinases in p15Ink4b-expressing cells

Transcription factors, including PU.1, are downstream targets of signal-transduction pathways. It has been shown that PU.1 is critical for DC development,<sup>34,35</sup> and its activity is regulated directly by protein kinase C  $\delta$  (PKC $\delta$ ) isoform and indirectly by Erk1/2 during cDC differentiation.<sup>23</sup> Therefore, we investigated the pathways through which p15Ink4b could modulate the transcriptional activity of PU.1 downstream of the LPS ligand TLR4 signaling in RAW264.7 cells. Expression of TLR4 and an important downstream mediator, MyD88, were not affected by DDp15 (Figure 7A). However, phosphorylation of Erk1/Erk2 was elevated in DDp15-expressing cells compared with control cells. Elevated phosphorylation of Erk1/2 was detected even before stimulation with LPS and persisted significantly longer after LPS stimulation in cells expressing DDp15 (Figure 7B). Signal transduction through another MAPK pathway, as judged by phosphorylation of p38Mapk, was not affected (Figure 7B). PKC $\delta$  has been shown to phosphorylate and activate PU.1 in human BM-DCs.<sup>23</sup> Therefore, we investigated the phosphorylation status of PKC $\delta$ . Results from Western blot analysis revealed that PKC $\delta$  was constitutively phosphorylated in RAW264.7 cells (Figure 7C). To confirm these data in primary cells, we sorted p15Ink4b<sup>fl/fl</sup>-LysMcre BM-DCs infected with Mig0 or MigDDp15, treated them with LPS, and performed Western blot analysis. Consistent with our previous results, increased and longer-lasting phosphorylation of Erk1/2 in response to LPS were detected in BM-DCs expressing the p15Ink4b protein (Figure 7D). We also detected slightly increased phosphorylation of PKC $\delta$  in BM-DCs expressing DDp15 compared with control cells. Furthermore, inhibition of Erk1/2 phosphorylation (Figure 7E) resulted in decreased transcriptional activity of PU.1 (Figure 7F) and suppression of the target genes CD80 and CD86 (Figure 7G), even in the presence of DDp15. These results suggest that p15Ink4b positively affects the differentiation and maturation of cDCs at least in part through increased Erk1/2 signaling. This is required for an optimal activity of the PU.1 transcription factor that is absolutely essential for the proper development and maturation of DCs.<sup>33-35</sup>

### Discussion

In the present study, we provide evidence for a novel role of p15Ink4b in the development of cDCs. Using knockout mice, we have shown that p15Ink4b affects cDC development in 2 separate steps. First, early during DC development, p15Ink4b expression positively modulates CDP differentiation from hematopoietic progenitors, because mice deficient in p15Ink4b had significantly lower numbers of CDPs compared with wild-type animals. We also uncovered a second role for p15Ink4b during late stages of maturation and activation of cDCs, in which the presence of p15Ink4b accelerates maturation and regulates the expression of several surface molecules required for the immunostimulatory function of cDCs. This 2-fold function of p15Ink4b is also supported by the biphasic induction of its expression, first during differentiation and later during maturation/activation of BM-DCs.

We showed previously that deletion of p15Ink4b results in increased numbers of GMPs at the expense of megakaryocyte/erythroid progenitors, causing mice to develop nonreactive monocytes as they aged.<sup>5,8</sup> Interestingly, this early function for p15Ink4b during the differentiation of progenitors seems to be

cell-cycle independent, because CMPs and GMPs from wild-type or knockout mice proliferate at comparable rates.<sup>8</sup> The present results also do not reveal any significant difference in the proliferation of DC progenitors isolated from wild-type or knockout mice. It was reported recently that treatment of hematopoietic progenitors with TGF- $\beta$  shifts the differentiation of CDPs toward cDCs through the induction of instructive factors for cDC development and the inhibition of factors necessary for pDC development.<sup>36</sup> Considering that p15Ink4b is a known downstream target of TGF- $\beta$  treatment,<sup>37</sup> our present observations suggest that p15Ink4b is one of the important effectors of TGF- $\beta$  signaling that modulate cDC development. This is supported by our observations that the steady-state levels of splenic and BM CD8<sup>-</sup> cDCs were also negatively affected by the deletion of *p15Ink4b*, whereas pDCs and CD8<sup>+</sup> cDC numbers were not.

One hallmark of immature DCs is their ability to acquire soluble antigen from their surrounding environment continuously.<sup>38,39</sup> We show herein that p15Ink4b is implicated in the endocytic activity of cDCs. Experiments with OVA peptide reveal a decreased ability to uptake antigen by BM-DCs lacking p15Ink4b. Efficient endocytosis is an essential step that transforms DCs from cells specialized in phagocytic uptake into immunostimulatory cells that present antigen and prime naive T cells.<sup>40</sup> Interestingly, deletion of *p15Ink4b* also resulted in decreased populations of naive splenic cDCs that expressed significantly lower levels of MHC I and MHC II molecules, which are necessary for antigen presentation. Furthermore, BM-DCs from floxed mice failed to mature appropriately after stimulation with LPS, as judged by their significantly reduced expression of CD80 and CD86. This partial maturation of cDCs was further confirmed by their impaired ability to stimulate allogeneic T-cell proliferation. These data suggest that p15Ink4b plays a crucial role in the differentiation and maturation processes of cDCs.

Although *p15Ink4b* loss is tightly associated with the development of AML and MDS<sup>1,2</sup> and has been proven experimentally to be a tumor suppressor in myeloid malignancies,<sup>5</sup> its role in disease progression has not been fully addressed. Our present results suggest that *p15Ink4b* loss may also promote a favorable environment for preleukemic cells to avoid immune clearance during disease progression by impairing the development of mature, immunostimulatory cDCs capable of efficient priming of naive T cells. Interestingly, reintroduction of exogenous p15Ink4b into BM-DCs derived from knockout mice restored the expression of cell-surface molecules, and this may have an important practical implication for DC-based immunotherapies for AML patients. DCs generated from AML blasts have been shown to retain the leukemia-associated antigens of the leukemic clone and are considered to be promising candidates for future vaccination strategies.<sup>41</sup> However, the generation of immunostimulatory DCs from leukemic blasts has been shown to vary widely from patient to patient, and the efficacy of this approach is also limited by the intrinsic abnormalities of the blasts that affect the differentiation of DCs.<sup>42,43</sup> In the present study, we present evidence that restored p15Ink4b expression in murine BM cells strongly increases the generation of CD11c<sup>+</sup>/CD11b<sup>+</sup> BM-DCs with a mature phenotype. Based on our results and the observation that *p15Ink4b* expression is silenced by methylation in more than 80% of all AML subtypes, reexpression of this gene using demethylating drugs may lead to significant improvement of DC-based vaccines prepared from AML patients. This hypothesis is supported by a recent study in which blasts from AML patients treated with a DNA hypomethylating agent 5-azacytidine generated DCs with improved cytokine profile and

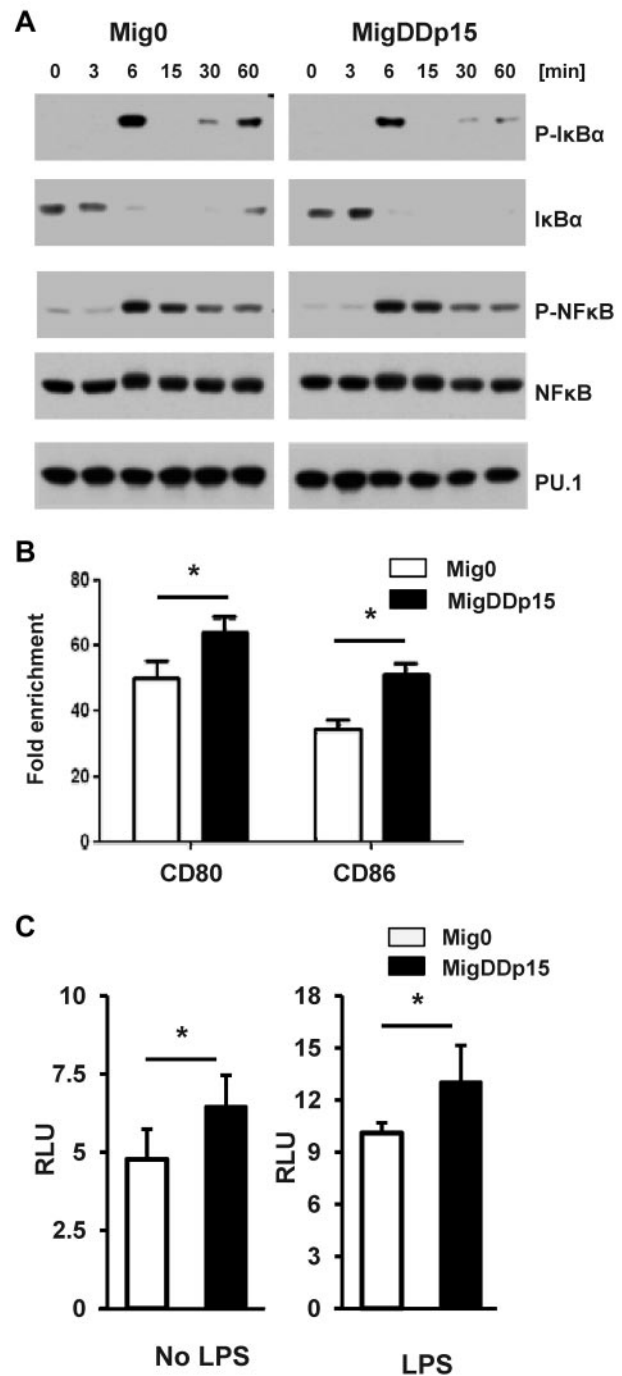
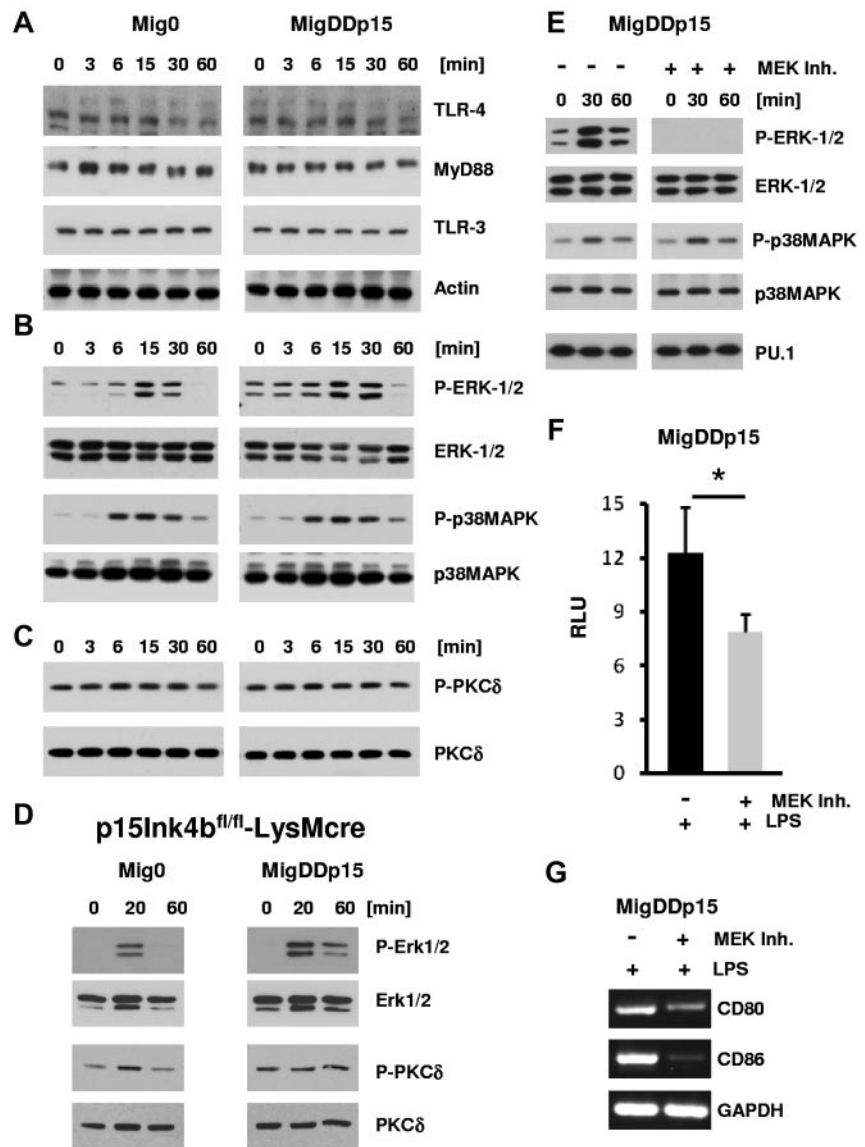


**Figure 6. Increased transcriptional activity of PU.1 in cells expressing p15Ink4b.** (A) Cell lysates from RAW264.7 cells expressing empty vector (Mig0) or p15Ink4b (MigDDp15) and treated with LPS (1  $\mu$ g/mL) for the indicated periods were analyzed by Western blot with Abs against the indicated phosphorylated I $\kappa$ B $\alpha$  (Ser-32) or NF- $\kappa$ Bp65 (Ser536) and the total I $\kappa$ B $\alpha$ , NF- $\kappa$ Bp65, and PU.1 (Cell Signaling Technology) proteins. The representative results shown are from the same blot that was stripped and reprobed with anti-actin. (B) Binding of PU.1 to the CD80 or CD86 promoter in RAW264.7 cells was evaluated by ChIP assay using qPCR. Results were normalized to histone H3 ChIPs and are plotted as the -fold enrichment over the normal IgGs. (C) Transcriptional activity of PU.1 was evaluated by dual luciferase reporter assay in RAW264.7 cells transfected with the PU.1-dependent luciferase reporter pPU.1-Luc construct and the *Renilla* luciferase pCMV-RL construct. Twenty-four hours after transfection, cells were either treated or untreated with LPS (1  $\mu$ g/mL) for another 12 hours, then lysed and analyzed for luciferase activity by luminometry. Data are shown as means  $\pm$  SD from 2 independent experiments. \* $P$  < .05.

immunostimulatory activity.<sup>44</sup> We and others have shown that 5-azacytidine treatment successfully reexpresses methylation-silenced *p15Ink4b* in blasts isolated from AML patients and



**Figure 7. Elevated Erk signaling in cells expressing p15Ink4b.** RAW264.7-Mig0 or RAW264.7-MigDDp15 cells were treated with LPS (1  $\mu$ g/mL) for the indicated times, lysed, and analyzed by Western blot with Abs against TLR4 (Abgent Technologies); MyD88 and TLR3 (Cell Signaling Technology) and actin (Santa Cruz Biotechnology; A); phospho-Erk1/2(Thr202/Tyr204), Erk1/2, phospho-p38MAPK (Thr180/Tyr182), and p38MAPK (Cell Signaling Technology; B); and phospho-PKC $\delta$  (Thr505) and PKC $\delta$  (Cell Signaling Technology; C). (D) BM-DCs generated from p15Ink4b<sup>fl/fl</sup>-LysMcre BM progenitors infected with Mig- or MigDDp15-expressing retroviruses were treated with LPS (100 ng/mL) for the indicated times and analyzed by Western blot with the specified Abs. (E) RAW264.7-MigDDp15 cells were pretreated with MEK1/2 inhibitor UO126 (5  $\mu$ M) for 30 minutes before treatment with LPS (1  $\mu$ g/mL) for the indicated times, lysed, and analyzed by Western blot. The representative results shown are from the same membrane that was stripped and reprobed. (F) Luciferase reporter assay for PU.1 was evaluated as described in Figure 6C. RAW264.7-MigDDp15 cells either treated or untreated with UO126 (5  $\mu$ M) and LPS (1  $\mu$ g/mL) for 24 hours were lysed and analyzed by luminometry. (G) Expression of CD80, CD86, and GAPDH mRNAs in RAW264.7-MigDDp15 cells treated or not with UO126 and LPS as indicated for 6 hours. Data are shown as means  $\pm$  SD from 2 independent experiments. \**P* < .05.



myeloid cell lines.<sup>45,46</sup> However, whereas the presented results in murine primary cells and our preliminary results with human AML-derived cell lines (supplemental Figure 4) support a potential clinical application for immunotherapy, a large experimental study with primary blasts isolated from AML patients with and without silenced (methylated) *p15INK4b* is required to validate this assumption.

On the molecular level, we have shown herein that the transcription factor PU.1 is an important downstream target through which p15Ink4b regulates cDC development and maturation. In agreement with what we observed in *p15Ink4b* knockout mice, PU.1-deficient mice also failed to develop CD8 $\alpha$ <sup>-</sup>cDCs in vivo and in vitro, whereas the CD8 $\alpha$ <sup>+</sup>cDCs remained uncompromised.<sup>34</sup> Recently, Carrota et al<sup>35</sup> showed that whereas PU.1 activity is absolutely necessary for the development of both cDCs and pDCs, higher activity of PU.1 is required for development of cDCs than for pDCs. Accordingly, mice heterozygous for PU.1 had significantly decreased numbers of cDCs, whereas pDCs were not affected. This is in a good agreement with our present results showing that the lack of p15Ink4b expression results in lower activity of PU.1 and a concomitant decreased production of

CD8<sup>-</sup>cDCs, whereas the development of pDCs was not reduced. Furthermore, increased levels of PU.1 are also found to be necessary for monocyte commitment into the DC lineage,<sup>47</sup> and the expression of several PU.1 targets, such as CD80, CD86, TNF- $\alpha$ , CD40, and MHC II,<sup>22,48-50</sup> is also decreased in BM-DCs derived from *p15Ink4b*-knockout mice, providing additional evidence for a functional cooperation between PU.1 and p15Ink4b.

It has been shown recently that the transcriptional activity of PU.1 in BM-DCs depends on the activities of Erk1/2 and PKC $\delta$  kinases. Furthermore, whereas PKC $\delta$  phosphorylates PU.1 directly, Erk kinases modulate its activity indirectly, probably through phosphorylation of an unknown PU.1 cofactor.<sup>23</sup> The significantly increased phosphorylation of Erk1/2 kinases in a p15Ink4b-expressing cell line and in primary BM-DCs suggests that p15Ink4b regulates the activity of PU.1 through the Erk-signaling pathway. However, the exact molecular mechanism through which p15Ink4b affects Erk signaling is not known presently and further experiments are warranted.

We showed previously that p15Ink4b is directly regulated by PU.1 in myeloid cells.<sup>7</sup> In the present study, we provide the proof that p15Ink4b can positively modulate the activity of the PU.1

transcription factor. This mutual regulation creates a positive feedback loop that results in amplification of the DC differentiation signal.

In summary, in the present study, we provide evidence for a novel function for the tumor suppressor p15Ink4b in cDC development. We also suggest that p15Ink4b, through regulation of the differentiation and maturation of cDCs, may serve as an important controller of adaptive immunity.

## Acknowledgments

The authors thank Mary Albaugh (National Cancer Institute [NCI], NIH, Frederick, MD) for excellent animal care, Barbara Taylor and Subhadra Banerjee (FACS Core Facility, NCI, NIH, Bethesda, MD) for technical assistance and advice with FACS, Cynthia Dunbar (National Heart, Lung, and Blood Institute, NIH, Bethesda,

MD) for providing human CD34<sup>+</sup> cells, and Egbert Flory (Paul Ehrlich-Institut, Germany) for providing the pPU.1-Luc construct.

This work was supported by the Intramural Research Program of the Center for Cancer Research, NCI, NIH (Bethesda, MD).

## Authorship

Contribution: J.F. designed and performed the research, analyzed the data, and wrote the manuscript; R.K. and R.H. performed the research; L.W. designed the research and edited the manuscript; and J.B. designed and performed the research, analyzed and interpreted the data, and wrote the manuscript.

Conflict-of-interest disclosure: The authors declare no competing financial interests.

Correspondence: Juraj Bies, NCI, NIH, Bldg 37/4124, 37 Convent Dr, Bethesda, MD 20892; e-mail: biesj@mail.nih.gov.

## References

- Herman JG, Jen J, Merlo A, Baylin SB. Hypermethylation-associated inactivation indicates a tumor suppressor role for p15INK4B. *Cancer Res*. 1996;56(4):722-727.
- Cameron EE, Baylin SB, Herman JG. p15(INK4B) CpG island methylation in primary acute leukemia is heterogeneous and suggests density as a critical factor for transcriptional silencing. *Blood*. 1999;94(7):2445-2451.
- Quesnel B, Guillem G, Vereecque R, et al. Methylation of the p15(INK4b) gene in myelodysplastic syndromes is frequent and acquired during disease progression. *Blood*. 1998;91(8):2985-2990.
- Uchida T, Kinoshita T, Nagai H, et al. Hypermethylation of the p15INK4B gene in myelodysplastic syndromes. *Blood*. 1997;90(4):1403-1409.
- Bies J, Sramko M, Fares J, et al. Myeloid-specific inactivation of p15Ink4b results in monocytosis and predisposition to myeloid leukemia. *Blood*. 2010;116(6):979-987.
- Ortega S, Malumbres M, Barbacid M. Cyclin D-dependent kinases, INK4 inhibitors and cancer. *Biochim Biophys Acta*. 2002;1602(1):73-87.
- Schmidt M, Bies J, Tamura T, Ozato K, Wolff L. The interferon regulatory factor ICSBP/IRF-8 in combination with PU.1 up-regulates expression of tumor suppressor p15(Ink4b) in murine myeloid cells. *Blood*. 2004;103(11):4142-4149.
- Rosu-Myles M, Taylor BJ, Wolff L. Loss of the tumor suppressor p15Ink4b enhances myeloid progenitor formation from common myeloid progenitors. *Exp Hematol*. 2007;35(3):394-406.
- Banchereau J, Steinman RM. Dendritic cells and the control of immunity. *Nature*. 1998;392(6673):245-252.
- Steinman RM, Hawiger D, Nussenzweig MC. Tolerogenic dendritic cells. *Annu Rev Immunol*. 2003;21:685-711.
- Merad M, Manz MG. Dendritic cell homeostasis. *Blood*. 2009;113(15):3418-3427.
- Naik SH, Sathe P, Park HY, et al. Development of plasmacytoid and conventional dendritic cell subtypes from single precursor cells derived in vitro and in vivo. *Nat Immunol*. 2007;8(11):1217-1226.
- Onai N, Obata-Onai A, Schmid MA, Ohteki T, Jarrossay D, Manz MG. Identification of clonogenic common Flt3+M-CSFR+ plasmacytoid and conventional dendritic cell progenitors in mouse bone marrow. *Nat Immunol*. 2007;8(11):1207-1216.
- Gabrilovich DI, Ciernik IF, Carbone DP. Dendritic cells in antitumor immune responses. I. Defective antigen presentation in tumor-bearing hosts. *Cell Immunol*. 1996;170(1):101-110.
- Almand B, Resser JR, Lindman B, et al. Clinical significance of defective dendritic cell differentiation in cancer. *Clin Cancer Res*. 2000;6(5):1755-1766.
- Latres E, Malumbres M, Sotillo R, et al. Limited overlapping roles of P15(INK4b) and P18(INK4c) cell cycle inhibitors in proliferation and tumorigenesis. *EMBO J*. 2000;19(13):3496-3506.
- Inaba K, Inaba M, Romani N, et al. Generation of large numbers of dendritic cells from mouse bone marrow cultures supplemented with granulocyte/macrophage colony-stimulating factor. *J Exp Med*. 1992;176(6):1693-1702.
- Lutz MB, Kukulski N, Ogilvie AL, et al. An advanced culture method for generating large quantities of highly pure dendritic cells from mouse bone marrow. *J Immunol Methods*. 1999;223(1):77-92.
- Liebermann DA, Hoffman-Liebermann B. Proto-oncogene expression and dissection of the myeloid growth to differentiation developmental cascade. *Oncogene*. 1989;4(5):583-592.
- Wells AD, Gudmundsdottir H, Turka LA. Following the fate of individual T cells throughout activation and clonal expansion. Signals from T cell receptor and CD28 differentially regulate the induction and duration of a proliferative response. *J Clin Invest*. 1997;100(12):3173-3183.
- Livak K, Schmittgen T. Analysis of Relative Gene Expression Data using Real Time Quantitative PCR and the 2-delta-deltaCT method. *Methods*. 2001;25(4):402-408.
- Kanada S, Nishiyama C, Nakano N, et al. Critical role of transcription factor PU.1 in the expression of CD80 and CD86 on dendritic cells. *Blood*. 2011;117(7):2211-2222.
- Hamdorf M, Berger A, Schule S, Reinhardt J, Flory E. PKCdelta-induced PU.1 phosphorylation promotes hematopoietic stem cell differentiation to dendritic cells. *Stem Cells*. 2011;29(2):297-306.
- Sallusto F, Lanzavecchia A. Efficient presentation of soluble antigen by cultured human dendritic cells is maintained by granulocyte/macrophage colony-stimulating factor plus interleukin 4 and downregulated by tumor necrosis factor alpha. *J Exp Med*. 1994;179(4):1109-1118.
- Onai N, Manz MG, Schmid MA. Isolation of common dendritic cell progenitors (CDP) from mouse bone marrow. *Methods Mol Biol*. 2010;595:195-203.
- Santambrogio L, Sato AK, Carven GJ, Belyanskaya SL, Strominger JL, Stern LJ. Extracellular antigen processing and presentation by immature dendritic cells. *Proc Natl Acad Sci U S A*. 1999;96(26):15056-15061.
- Santambrogio L, Sato AK, Fischer FR, Dorf ME, Stern LJ. Abundant empty class II MHC molecules on the surface of immature dendritic cells. *Proc Natl Acad Sci U S A*. 1999;96(26):15050-15055.
- Haugwitz M, Nourzaie O, Gandlur S, Sagawa H. ProteoTuner: a novel system with rapid kinetics enables reversible control of protein levels in cells and organisms. *BioTechniques*. 2008;44(3):432-433.
- Saxena RK, Vallyathan V, Lewis DM. Evidence for lipopolysaccharide-induced differentiation of RAW264.7 murine macrophage cell line into dendritic like cells. *J Biosci*. 2003;28(1):129-134.
- Lee YN, Lee HY, Kang HK, Kwak JY, Bae YS. Phosphatidic acid positively regulates LPS-induced differentiation of RAW264.7 murine macrophage cell line into dendritic-like cells. *Biochem Biophys Res Commun*. 2004;318(4):839-845.
- Burkly L, Hession C, Ogata L, et al. Expression of relB is required for the development of thymic medulla and dendritic cells. *Nature*. 1995;373(6514):531-536.
- Wu L, D'Amico A, Winkel KD, Suter M, Lo D, Shortman K. RelB is essential for the development of myeloid-related CD8alpha-dendritic cells but not of lymphoid-related CD8alpha+ dendritic cells. *Immunity*. 1998;9(6):839-847.
- Anderson KL, Perkin H, Surh CD, Venturini S, Maki RA, Torbett BE. Transcription factor PU.1 is necessary for development of thymic and myeloid progenitor-derived dendritic cells. *J Immunol*. 2000;164(4):1855-1861.
- Guerriero A, Langmuir PB, Spain LM, Scott EW. PU.1 is required for myeloid-derived but not lymphoid-derived dendritic cells. *Blood*. 2000;95(3):879-885.
- Carotta S, Dakic A, D'Amico A, et al. The transcription factor PU.1 controls dendritic cell development and Flt3 cytokine receptor expression in a dose-dependent manner. *Immunity*. 2010;32(5):628-641.
- Felker P, Sere K, Lin Q, et al. TGF-beta1 accelerates dendritic cell differentiation from common dendritic cell progenitors and directs subset specification toward conventional dendritic cells. *J Immunol*. 2010;185(9):5326-5335.
- Hannon GJ, Beach D. p15INK4B is a potential effector of TGF-beta-induced cell cycle arrest. *Nature*. 1994;371(6494):257-261.
- Steinman RM. The dendritic cell system and its role in immunogenicity. *Annu Rev Immunol*. 1991;9:271-296.
- Austyn JM. Antigen uptake and presentation by dendritic leukocytes. *Semin Immunol*. 1992;4(4):227-236.

40. Inaba K, Steinman RM, Van Voorhis WC, Muramatsu S. Dendritic cells are critical accessory cells for thymus-dependent antibody responses in mouse and in man. *Proc Natl Acad Sci U S A*. 1983;80(19):6041-6045.
41. Choudhury BA, Liang JC, Thomas EK, et al. Dendritic cells derived in vitro from acute myelogenous leukemia cells stimulate autologous, anti-leukemic T-cell responses. *Blood*. 1999;93(3):780-786.
42. Kharfan-Dabaja M, Ayala E, Lindner I, et al. Differentiation of acute and chronic myeloid leukemic blasts into the dendritic cell lineage: analysis of various differentiation-inducing signals. *Cancer Immunol Immunother*. 2005;54(1):25-36.
43. Cignetti A, Bryant E, Allione B, Vitale A, Foa R, Cheever MA. CD34(+) acute myeloid and lymphoid leukemic blasts can be induced to differentiate into dendritic cells. *Blood*. 1999;94(6):2048-2055.
44. Frikeche J, Clavert A, Delaunay J, et al. Impact of the hypomethylating agent 5-azacytidine on dendritic cells function. *Exp Hematol*. 2011;39(11):1056-1063.
45. Paul TA, Bies J, Small D, Wolff L. Signatures of polycomb repression and reduced H3K4 trimethylation are associated with p15INK4b DNA methylation in AML. *Blood*. 2010;115(15):3098-3108.
46. Berg T, Guo Y, Abdelkarim M, Fliegau M, Lubbert M. Reversal of p15/INK4b hypermethylation in AML1/ETO-positive and -negative myeloid leukemia cell lines. *Leuk Res*. 2007;31(4):497-506.
47. Dakic A, Wu L, Nutt SL. Is PU.1 a dosage-sensitive regulator of haemopoietic lineage commitment and leukaemogenesis? *Trends Immunol*. 2007;28(3):108-114.
48. Fukai T, Nishiyama C, Kanada S, et al. Involvement of PU.1 in the transcriptional regulation of TNF-alpha. *Biochem Biophys Res Commun*. 2009;388(1):102-106.
49. Nguyen VT, Benveniste EN. Involvement of STAT-1 and ets family members in interferon-gamma induction of CD40 transcription in microglia/macrophages. *J Biol Chem*. 2000;275(31):23674-23684.
50. Ito T, Nishiyama C, Nakano N, et al. Roles of PU.1 in monocyte- and mast cell-specific gene regulation: PU.1 transactivates CIITA pIV in cooperation with IFN-gamma. *Int Immunol*. 2009;21(7):803-816.